

## Surface Distribution of Iron and Chromium on 84 Ursae Majoris

JOHN RICE<sup>1</sup>

Department of Physics and Astronomy, Brandon University, Brandon, Manitoba R7A 6A9, Canada  
 Electronic mail: rice@brandonu.ca

WILLIAM WEHLAU<sup>1</sup>

Department of Astronomy, University of Western Ontario, London, Ontario N6M 1Z0, Canada  
 Electronic mail: whwehla@uwo.ca

Received 1993 August 2; accepted 1993 November 10

**ABSTRACT.** High-resolution spectra of 84 Ursae Majoris have been used to map the surface distributions of iron and chromium. The abundances of iron and chromium on the surface varied by a factor of 15. Iron is less abundant than in the solar atmosphere, by about a factor of 0.6 in the maximum areas, while chromium is more abundant than in the Sun, by about a factor 600 in the minimum areas; the abundances are compared with those for three other CP stars previously studied. The best fit of the computed line profiles to the observed ones was obtained using a microturbulent velocity of  $4 \text{ km s}^{-1}$ ; such broadening may be due to the Zeeman effect of an undetected magnetic field. Although the surface distributions show some regular structure, no symmetries similar to those found for other stars with dipolar magnetic fields are apparent.

### 1. INTRODUCTION

The star 84 Ursae Majoris (HR 5187, HD 120198, SAO 28885) is a spectrum variable, classified as B9pEuCr in the *Bright Star Catalog* (Hoffleit 1982). Although there is considerable blending of the spectral lines due to rotational broadening, the most uncontaminated lines were judged to be suitable to include the star in our program of mapping the surfaces of Ap stars.

Measurements of the magnetic field of 84 UMa were made by Landstreet and Borra (1980). Only three observations were obtained, ranging from  $-380$  to  $+240$  G, but the standard deviations are of comparable size. A recent measurement (Hill 1993) with the UWO 1.2-m telescope gave  $215 \pm 325$  G. The only conclusion which can be drawn at this time is that there is no evidence for a large magnetic field. The photometric variability is discussed below. Bonsack (1974) briefly discussed the spectral variations which he observed on four photographic spectrograms. Adelman (1980) measured the energy distribution and the variations in it. The effective temperature is given by Stepien and Dominiczak (1989) as 10,100 K.

### 2. THE PERIOD

The photometric variability of 84 UMa has been studied most recently by Burke and Barr (1981). Combining their data with earlier observations by Winzer, they gave the ephemeris as  $\text{HJD } (U_{\text{max}}) = 2441444.80 + 1.37996E$ . The amplitude in  $U$  is about 0.04 mag, while in  $B$  and  $V$  the amplitude is much smaller.

A periodogram of all the  $U$  observations gives a maxi-

mum at that same period. A graph of the  $U$  observations with that period produces a satisfactory light curve. However, one point, JD 244114.723, from Winzer's (1974) data falls about 0.048 mag below the mean curve while all other points deviate by less than 0.015 mag. A periodogram of all the  $U$  observations, except that one point gives a maximum at a period of 1.380682 days. This period also produces a satisfactory light curve, with a variance per point of  $3.3 \text{ exp } -5$ , slightly smaller than that of  $4.0 \text{ exp } -5$  for a period of 1.37996. Consequently we have adopted the period of 1.380682 days to compute the phases of our spectroscopic observations, and an ephemeris  $\text{HJD } (U_{\text{max}}) = 2441445.004 + 1.380682E$ . Although this appears to be the best solution given the photometric data available, several aliases have peaks in the periodogram comparable with the one adopted.

### 3. OBSERVATIONS

High-resolution spectra of 84 UMa were obtained in 1989 and 1990 using the Canada–France–Hawaii telescope with the coudé spectrograph and a Reticon detector. The resolution was  $0.09 \text{ \AA}$ ; a more detailed description, including the instrumental profile, has been given earlier (Rice and Wehla 1982). Exposure times were generally about 30 to 40 min, approximately 0.02 of the period or less.

Each observation covered about  $60 \text{ \AA}$  of the spectrum. Two regions were observed, centered at 4550 and at 4920  $\text{ \AA}$ . The spectra used for the mapping are listed in Table 1. Figure 1 shows profiles of the  $\lambda 4523 \text{ Fe II}$  line. The crosses are the observed values, the dashed line was computed from the map obtained as the solution of the inverse problem when the observed spectra were used as input.

<sup>1</sup>Visiting Astronomer: Canada–France–Hawaii Telescope, operated by the National Research Council of Canada, the Centre National de la Recherche Scientifique de France, and the University of Hawaii.

TABLE 1  
Dates and Phases of Observations

$\lambda$ 4550		$\lambda$ 4920	
JD - 2440000	Phase	JD - 2440000	Phase
1989			
7637.9722	0.589	7637.9023	0.538
7638.8055	0.192	7638.8669	0.237
7638.9674	0.310	7641.0446	0.814
7640.9438	0.741		
7641.0903	0.848		
1990			
7994.7944	0.028	7994.8553	0.072
7994.9722	0.157	7995.0651	0.224
7995.7958	0.754	7995.8671	0.805
7995.9868	0.892	7996.0893	0.966
7996.7660	0.456	7996.8324	0.504
7996.9257	0.572	7996.9935	0.621
7997.0514	0.663	7997.8310	0.228
7997.7188	0.146	7998.0511	0.387
7997.9500	0.314		
7998.1021	0.424		

#### 4. SOLUTION OF THE INVERSE PROBLEM

The solution of the inverse problem to produce maps of the surface distributions of the abundances was carried out as described previously to Rice and Wehlau (1991) and references therein. We produce separate maps (also referred to as Images) from individual lines, and then average them. To compute the local line profiles we used the Kurucz (1979) model atmosphere with  $\log g=4.0$  and  $T_e=11,000$  K.

Line blending was a major problem in mapping this star. Although blended lines can be used for the solution of the inverse problem, that seemed inappropriate here. The observed lines are quite shallow. The identifications of some of the blending lines are uncertain, which does not allow us to treat them as constant lines, lines due to an element being mapped, or other variable lines. The lines from which maps were produced are listed in Table 2.

The spectral lines were described by Babcock (1958) as broad ( $w=1.0$ ). In Durrant's list (1970) the value of

TABLE 2  
Parameters of Lines Used for the Maps

Line ( $\text{\AA}$ )	Ion	Log(gf)	E.P. (eV)	Comments
Chromium				
4896.083	II	-2.74	6.48	
4901.650	II	-1.17	6.48	
4948.641	I	+0.80	3.41	Cr ?
4558.660	II	-0.69	4.07	
Iron				
4520.217	II	-3.09	2.807	
4522.624	II	-2.22	2.844	
4923.921	II	-1.56	2.89	blending
4927.42	I	-0.44	3.57	

$V_e \sin i$  is listed as  $20 \text{ km s}^{-1}$ , the *Bright Star Catalog* gives  $37 \text{ km s}^{-1}$ , and Landstreet and Borra (1980) give  $45 \text{ km s}^{-1}$ . The line profiles in our spectra correspond to a substantially larger value. To obtain an adequate representation of our observed line profiles, a value near  $65 \text{ km s}^{-1}$  is required.

Initially we estimated  $V_e$  and  $i$  by computing a number of maps of iron with different values of  $V_e$  and of  $i$ , and looking for the values which minimized the discrepancies between the observed and computed line profiles. The minimum discrepancy was not sharply defined and occurred for  $i$  near  $60^\circ$  and  $V_e$  near  $72 \text{ km s}^{-1}$ , which implies a radius of the star of  $1.96R_\odot$ . Since this is quite a low value for  $R$ , we chose to adopt a radius of  $2.5R_\odot$  based on the spectral classification, although there is some uncertainty in the luminosity classification. This leads to  $V_e=92 \text{ km s}^{-1}$ , and to keep the  $V_e \sin i$  at a value near  $65 \text{ km s}^{-1}$  we need to adopt  $i=45^\circ$ . These values were used to produce the maps of the distributions of iron and chromium discussed below.

#### 5. DISCUSSION

Maps were produced from the profiles of each of the lines listed in Table 2. Each map gave the distribution of iron or chromium over the surface of 84 UMa. When considering the maps, the limitations of the Doppler Imaging procedure should be taken into account. Features near and below the star's equator are poorly reproduced or absent. This effect is intrinsic in the data as has been demonstrated in a number of papers where artificial stellar surfaces have been used to produce spectra which are then used in the solution of the inverse problem to produce maps for comparison with the original surface (Rice et al. 1989). The inability to map reliably the region below the equator is particularly well shown by Figs. 3 and 4 in the paper by Piskunov and Wehlau (1990), where the map of that region remains at nearly the initially assumed abundance even when the map correctly reproduces the spectra. This limitation of Doppler Imaging arises because relatively large areas of the star, which are seen only briefly under considerable foreshortening, make only a small contribution to the observed spectra.

The variations in the spectral lines appear small, which may be attributed in part to the high  $V_e \sin i$  which smears out the line and distributes the effects of any local changes of abundance on the star over a relatively large range in

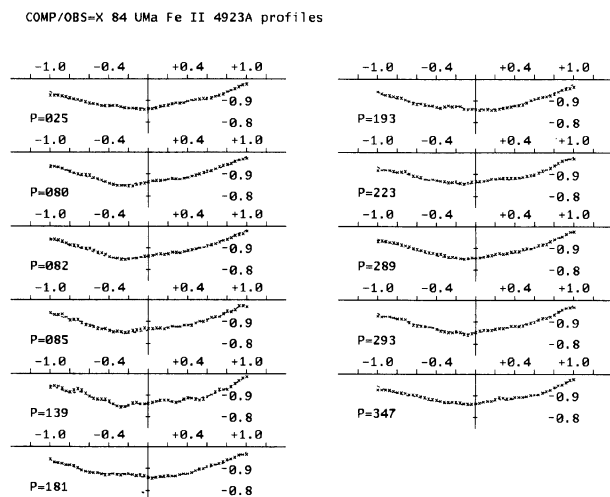


FIG. 1—Profiles of the  $\lambda 4923$  Fe II line. Crosses are the observed points. The solid line was computed from the distribution of iron obtained when the inverse problem was solved for the observed spectra.

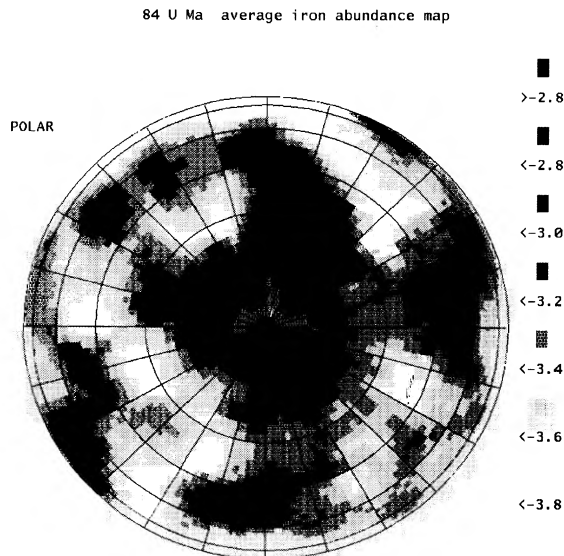


FIG. 2—The distribution of iron, with microturbulent velocity =  $4.0 \text{ km s}^{-1}$ .

wavelength in the line; this also makes the blending problem serious for this star. Hatzes (1993) found that apparent variations of the line profiles in his spectra of 84 UMa were quite weak, and that blending was severe. While the similarity of our iron and chromium maps, discussed below, implies that the observed line profile variations are due to the surface inhomogeneities shown in the maps, additional maps produced independently are desirable.

In computing local line profiles on the surface of the star, the macroturbulent velocity was taken to be  $0.0 \text{ km s}^{-1}$ . Initially the microturbulent velocity was taken as  $1.0 \text{ km s}^{-1}$ , consistent with work on other stars of this type. The fit of the line profiles computed from the derived maps to the observed spectra appeared to be less satisfactory than might be expected from the quality of the data. One possible source of the discrepancy is an undetected magnetic field. At present, our computer programs to solve the inverse problem do not include the effects of any magnetic field, so we have approximated the possible Zeeman broadening by increasing the microturbulent velocity.

The smallest discrepancy between the computed and observed line profiles was obtained for a microturbulent velocity of  $4 \text{ km s}^{-1}$ . For the lines used here, a  $1 \text{ kG}$  field will produce a Zeeman splitting of about  $1 \text{ km s}^{-1}$ . Of course, the suggestion, on this basis, that a substantial magnetic field is present is questionable because of the approximation of Zeeman splitting by microturbulent velocity, and the large ratio of  $V_e \sin i$  to the microturbulent velocity. In addition, a global field might be expected to produce a correspondingly simple distribution of iron and chromium, which is not observed. A more complicated magnetic field would be consistent with the iron and chromium distributions, and with the lack of detection of a magnetic field. Since only a few attempts have been made to detect and measure a magnetic field, additional obser-

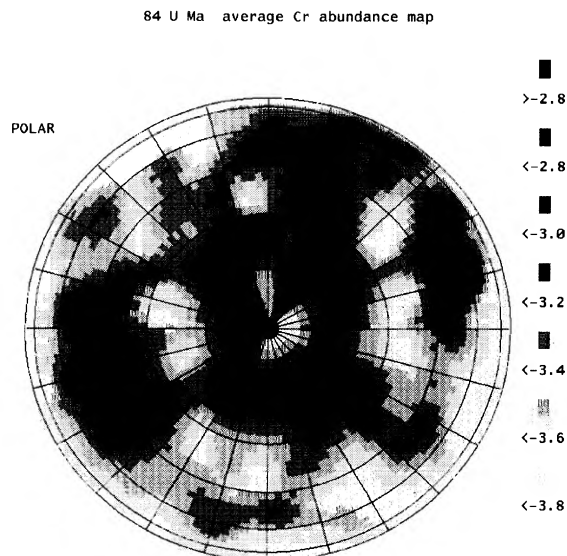


FIG. 3—The distribution of chromium.

vations with a hydrogen line polarimeter are planned.

The maps produced from individual lines were combined to give average maps of the distribution of iron and chromium on the surface of 84 UMa. These are presented in Figs. 2 and 3. The shading scale shown in each figure gives  $\log N/H$ , where  $N$  is the number of atoms of iron or chromium and  $H$  is the number of hydrogen atoms. The values for the solar atmosphere are  $-4.4$  for iron and  $-6.4$  for chromium. Over the surface of 84 UMa the abundance of iron varies by a factor of about 15, and is less abundant than in the solar atmosphere with the maximum at about 0.6 of the solar value. Chromium also varies by a factor of 15, but is more abundant in the atmosphere of 84 UMa than in the Sun, by about a factor of 600 in the minimum areas.

For comparison with several other stars which we have mapped previously, the abundances of iron and chromium are listed in Table 3. The values for  $\epsilon$  UMa and  $\theta$  Aurigae are from Rice and Wehlau (1991), for 21 Persei from Wehlau et al. 1991, and for the Sun from *Astrophysical Quantities* (Allen 1973). The values for 21 Per were derived in a somewhat different manner than that used here: maps of the equivalent widths were produced and the abundances then calculated from the equivalent widths. The ratio of high to low abundance on these CP stars ranges from 300 for chromium on  $\epsilon$  UMa to 30 on  $\theta$  Aur, and 15 on 84 UMa. Of these CP stars,  $\theta$  Aur has the

TABLE 3  
Abundances of Iron and Chromium

Star	Fe		Cr		SpType
	max	min	max	min	
84 UMa	-2.7	-3.9	-2.7	-3.9	B9pEuCr
$\epsilon$ UMa	-2.5	-4.8	-4.0	-6.5	A0pCr
$\theta$ Aur	-3.0	-4.5	-4.1	-5.6	A0pSi
21 Per	-3.0		-4.7		B9pSi
21 Per avg		-3.9		-5.4	
Sun		-4.41		-6.24	G2V

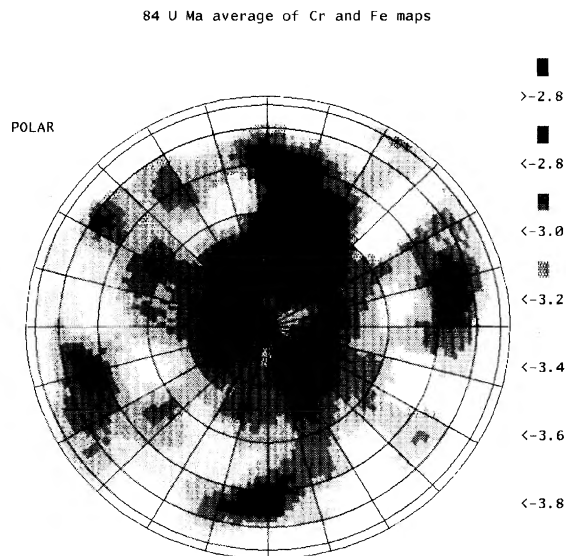


FIG. 4—The distribution of iron and chromium, obtained by averaging the maps of Figs. 2 and 3.

strongest measured magnetic field ( $-200$  to  $+400$  G, Borra and Landstreet 1980), while the largest ratio of high to low abundances is shown by  $\epsilon$  UMa, which has a field of only about 100 G (Bohlender and Landstreet 1990; Donati et al. 1990). The highest chromium abundance is found on 84 UMa, consistent with its classification as a chromium star.

The iron and chromium maps resemble each other and display some structure. If iron and chromium really have the same distribution, then the structure may be displayed more clearly in a map which is the average of the iron and chromium maps. Weighting the iron and chromium maps equally gives the average map shown in Fig. 4. None of

these maps shows the fairly obvious symmetries which we found for other stars such as  $\epsilon$  UMa, and  $\theta$  Aur (Rice and Wehlau 1991) which have magnetic fields dominated by the dipolar component. If 84 UMa has a more complicated field, it would be more difficult to detect, and the distribution of iron and chromium on the surface might also be more complicated.

The observations on which this paper is based were obtained at the Canada–France–Hawaii Telescope. Financial support was provided by the Natural Sciences and Engineering Council of Canada.

#### REFERENCES

- Adelman, S. J. 1980, *A&A*, 84, 149  
 Allen, C. W. 1973, *Astrophysical Quantities*, 3rd ed. (University of London, Athlone)  
 Babcock, H. W. 1958, *ApJS*, 3, 141  
 Bohlender, D. A., and Landstreet, J. D. 1990, *ApJ*, 358, L25  
 Bonsack, W. K. 1974, *PASP*, 86, 408  
 Borra, E. F., and Landstreet, J. D. 1980, *ApJS*, 42, 421  
 Burke, E. W., and Barr, T. H. 1981, *PASP*, 93, 344  
 Donati, J.-F., Semel, M., and del Toro Iniesta, J. C. 1990, *A&A*, 233, L17  
 Durrant, C. J. 1970, *MNRAS*, 147, 75  
 Hatzes, A. P. 1993, private communication  
 Hill, G. 1993, private communication  
 Hoffleit, D. 1982, *The Bright Star Catalog*, 4th revised ed. (New Haven, Yale University Observatory)  
 Kurucz, R. L. 1979, *ApJS*, 40, 1  
 Landstreet, J. D., and Borra, E. F. 1980, *ApJS*, 42, 421  
 Piskunov, N. E., and Wehlau, W. H. 1990, *A&A*, 233, 497  
 Rice, J. B., and Wehlau, W. H. 1991, *A&A*, 246, 195  
 Rice, J. B., and Wehlau, W. H. 1982, *A&A*, 106, 7  
 Rice, J. B., Wehlau, W. H., and Khokhlova, V. L. 1989, *A&A*, 208, 179  
 Stepién, K., and Dominiczak, R. 1989, *A&A*, 219, 197  
 Wehlau, W. H., Rice, J. B., and Khokhlova, V. L. 1991, *Astron. Astrophys. Trans.*, 1, 55  
 Winzer, J. E. 1974, Ph.D. thesis, University of Toronto